ORIGINAL ARTICLE

Open Access

An improved GNSS ambiguity best integer equivariant estimation method with Laplacian distribution for urban low-cost RTK positioning

Ying Liu[1], Wanke Liu[1*] , Xiaohong Zhang[1,2], Yantao Liang[1], Xianlu Tao[3] and Liye Ma[4,5]

Abstract

The integer least squares (ILS) estimation is commonly used for carrier phase ambiguity resolution (AR). More recently, the best integer equivariant (BIE) estimation has also attracted an attention for complex application scenarios, which exhibits higher reliability by a weighted fusion of integer candidates. However, traditional BIE estimation with Gaussian distribution (GBIE) faces challenges in fully utilizing the advantages of BIE for urban low-cost positioning, mainly due to the presence of outliers and unmodeled errors. To this end, an improved BIE estimation method with Laplacian distribution (LBIE) is proposed, and several key issues are discussed, including the weight function of LBIE, determination of the candidates included based on the OIA test, and derivation of the variance of LBIE solutions for reliability evaluation. The results show that the proposed LBIE method has the positioning accuracy similar to the BIE using multivariate t-distribution (TBIE), and significantly outperforms the ILS-PAR and GBIE methods. In an urban expressway test with a Huawei Mate40 smartphone, the LBIE method has positioning errors of less than 0.5 m in three directions and obtains over 50% improvements compared to the ILS-PAR and GBIE methods. In an urban canyon test with a low-cost receiver STA8100 produced by STMicroelectronics, the positioning accuracy of LBIE in three directions is 0.112 m, 0.107 m, and 0.252 m, respectively, with improvements of 17.6%, 27.2%, and 26.1% compared to GBIE, and 23.3%, 28.2%, and 30.6% compared to ILS-PAR. Moreover, its computational time increases by 30–40% compared to ILS-PAR and is approximately half of that using TBIE.

Keywords Ambiguity resolution, Best integer equivariant estimation, Laplacian distribution, Urban environments, Low-cost GNSS receivers, Real-time kinematic

*Correspondence:
Wanke Liu
wkliu@whu.edu.cn
[1] School of Geodesy and Geomatics, Hubei Luojia Laboratory, Wuhan University, 129 Luoyu Road, Wuhan 430079, Hubei, China
[2] Chinese Antarctic Center of Surveying and Mapping, Wuhan University, 129 Luoyu Road, Wuhan 430079, Hubei, China
[3] School of Instrument Science and Engineering, Southeast University, Nanjing, Jiangsu, China
[4] The 54, Research Institute of China Electronics Technology Group Corporation, Shijiazhuang 050081, Hebei, China
[5] State Key Laboratory of Satellite Navigation System and Equipment Technology, Shijiazhuang 050081, Hebei, China

Introduction

Fast and reliable carrier phase ambiguity resolution (AR) is crucial for accurate positioning of the Global Navigation Satellite System (GNSS), which is widely used in the fields involving navigation, positioning, and timing (PNT). Currently, GNSS has entered a new developmental stage, providing users with abundant satellite and frequency resources and enabling the realization of correct AR with a high success rate and high probability (Li, 2018; Odolinski & Teunissen, 2016). However, the challenge is that not all ambiguities can be reliably fixed and the efficiency of AR will also be decreased if more ambiguities are involved. Consequently, a partial ambiguity resolution (PAR) strategy has emerged to fix a subset of

the ambiguities and can significantly improve the reliability of AR (Teunissen et al., 1999). Nevertheless, diversified GNSS applications and different observation conditions often cause the gross errors and cycle slips in observations, which pose considerable challenges to reliable AR.

Integer ambiguity resolution (IAR) is typically solved using the integer least square (ILS) estimation, which has shown the highest success rate (Teunnissen, 1995; Xu et al., 2012). To perform IAR, a three-step procedure is usually included (Li & Wang, 2012): (a) ignore the integer characteristic of ambiguities, and calculate the float solution using least squares (LS) or kalman filter (KF) estimation, (b) fix the float ambiguity solution to integer values, and (c) update the float baseline solution using the fixed ambiguities and output the fixed solution. In the second step, it is essential to reject the incorrectly fixed ambiguities as much as possible to avoid severe bias in positioning. Over the past few decades, numerous efforts were made to enhance the validation test, which can be mainly categorized into three types: (a) the discrimination tests constructed with the quadratic form of ambiguity residuals (Euler & Schaffrin, 1991; Frei, 1990; Han, 1997; Tiberius & De Jonge, 1995; Wang et al., 1998), (b) the success or failure rate methods based on the theoretical framework of ambiguity estimation (Li et al., 2014; Verhagen et al., 2013), and (c) an integrated method combining both (Zhang et al., 2015). In fact, these methods can be unified into the class of integer aperture (IA) estimators, and the fail-rate can be controlled by setting the size and shape of the integer aperture pull-in region of an IA-estimator (Teunissen, 2003a). While these methods certainly reduce the acceptance of incorrectly fixed solutions, they have some challenges, such as the complexity of selecting critical values and the model's inconsistency with reality (Wu & Bian, 2015). It may lead to a low accuracy of float solution or the severe bias of incorrectly fixed solution, representing false-alarm and miss-detection errors, respectively. Especially in complex conditions with low-cost receivers, it is particularly evident when the float ambiguities are biased (Li et al., 2022).

Considering the difficulty in obtaining the correctly fixed solution, Teunissen (2003b) introduced the best integer equivariant (BIE) estimation as an alternative to AR, which is considered the best in the sense of minimizing mean squared error (MMSE) by making a weighted sum of all potential ambiguity candidates. Since it is propoed, many scholars have analyzed the performance of BIE. Verhagen and Teunissen (2005) initially validated the effectiveness of BIE estimation using simulation data. Afterwards, it was also assessed in GNSS relative positioning with the baselines of different lengths, and the results showed that it is comparable to the ILS fixed solution with a high success rate and superior to the ILS float solution with a low success rate (Odolinski & Teunissen, 2020). More recently, the BIE estimation has been applied to precision point positioning (PPP) and PPP-RTK (real-time kinematic) without external atmospheric corrections, significantly reducing convergence time and improving positioning accuracy (Brack et al., 2023; Yang et al., 2024). Additionally, Ma et al. (2022) used the optimal integer aperture (OIA) test to combine ILS and BIE, and Zhang et al. (2023a, 2023b) proposed the BIE estimation with quality control, further enhancing its performance in complex environments.

It is also a hot issue to study the effectiveness of BIE estimation from the probability distribution characteristics of GNSS observations. Teunissen (2003b) assumed the observations followed a Gaussian distribution and then derived an explicit expression. However, in urban environments with low-cost devices, receivers may experience high occlusion, strong reflection, and frequent maneuvers, which can lead to a decline in observation quality. Specifically, outliers and unmodeled errors, such as multipath and non-line-of-sight (NLOS) errors, are prominent, which induces a strong heavy-tailed effect, resulting in a higher probability of abnormal events and deviating the distribution characteristics of GNSS observations from Gaussian distribution. At this time, the BIE estimator derived from Gaussian distribution (GBIE) encounters a serious problem of model distortion. For example, the contamination of the float ambiguity solution leads to a mismatch in its smaller variance, generating large quadratic form of ambiguity residuals, which may lead to an irrational allocation of weight for candidates and impact the reliability of BIE. Fortunately, recent literature claims that using those heavy-tailed distributions aligns more closely with the actual error characteristics of GNSS observations and is an effective way to reduce incorrectly fixed ambiguities by spreading out the weights to other candidates. In this context, the BIE estimator using multivariate t-distribution (TBIE) has been proposed and its superiority was validated using both simulation and real-measured data (Duong et al., 2021; Odolinski & Teunissen, 2022; Teunissen, 2020). Additionally, Vollath and Talbot (2013) proposed the iFlex method in a patent to determine weights for candidates, which embodied the idea of Laplacian distribution. Duong et al. (2021) subsequently validated it using PPP and found that it has similar positioning accuracy and better efficiency compared to the multivariate t-distribution. In fact, the Laplace distribution is also considered a heavy-tailed distribution, exhibiting a greater prevalence of extreme values in its tails (Pisarenko & Rodkin, 2010). However, the current research on the BIE estimator using Laplacian distribution remains somewhat unclear, and its reliability and efficiency requires

further validation, especially for the data in urban environments with a higher incidence of outliers.

In this contribution, we propose an improved BIE estimation method with Laplacian distribution (LBIE) to enhance the urban low-cost positioning and discuss several key issues. Firstly, we analyze the limitations of GBIE and introduce the weight function for LBIE. Secondly, we formulate a criterion based on the OIA test to select the candidates included in the BIE estimation. Finally, we derive the variance–covariance (VC) matrix of LBIE solution to evaluate its reliability. Additionally, two real-measured vehicular experiments in urban environments were conducted to assess the performance of the proposed method. And then, we give the conclusions at the end.

Principle of GNSS integer ambiguity resolution

In a short baseline relative positioning model, the most errors in observations, including ionospheric and tropospheric delays, can be mitigated or even eliminated using the between-station and -satellite double-difference (DD) combination. The general linear equation of DD measurements can be formulated as:

$$E(y) = Aa + Bb, Q_{yy} = P_{yy}^{-1} \tag{1}$$

where y denotes the GNSS observations; $E(y)$ and Q_{yy} denote the mathematical expectation and VC matrix of y, respectively; P_{yy} denotes the corresponding weight matrix; a and b denote the integer-valued ambiguity and real-valued baseline vector, with $a \in Z^n$ and $b \in R^p$, respectively; A and B denote the corresponding coefficient matrices.

Integer least squares estimation.

The LS objective function to solve (1) can be formulated as:

$$\min_{a,b} ||y - Aa - Bb||^2_{Q_{yy}} \tag{2}$$

where $||\,||^2_Q = (\,)^T Q^{-1}(\,)$ represents the quadratic form of residuals. Due to the inclusion of both integer and real parameters, (2) is a mixed LS problem that cannot be directly solved by the conventional LS method. Here, the orthogonal decomposition method (Teunissen, 1993) is adopted and the objective function can be converted to the following form:

$$\breve{a} = \arg \min_{a \in Z^n} ||\hat{a} - \breve{a}||^2_{Q_{\hat{a}\hat{a}}} \tag{3}$$

where $\hat{a}$ and $\breve{a}$ denote the float and fixed ambiguity vectors, respectively; $Q_{\hat{a}\hat{a}}$ denotes the VC matrix of $\hat{a}$.

Generally, a three-step procedure is performed to solve the model (Li & Wang, 2012).

In step (a), ignore the integer characteristic of ambiguities, and calculate the float solution as:

$$\begin{bmatrix} \hat{a} \\ \hat{b} \end{bmatrix}, \begin{bmatrix} Q_{\hat{a}\hat{a}} & Q_{\hat{a}\hat{b}} \\ Q_{\hat{b}\hat{a}} & Q_{\hat{b}\hat{b}} \end{bmatrix} \tag{4}$$

In step (b), fix the float ambiguity solution to integer values. Assuming S is an n-dimensional mapping space, the fixed ambiguity vector can be expressed as:

$$\breve{a} = S(\hat{a}), S : R^n \to Z^n \tag{5}$$

The next is to validate the reliability of the fixed ambiguities. Among the three types of validation methods mentioned before, the R-ratio test is the most popular, which can be defined as Euler and Schaffrin (1991), Wang et al. (2017):

$$T = \frac{||\hat{a} - \breve{a}_2||^2_{Q_{\hat{a}\hat{a}}}}{||\hat{a} - \breve{a}_1||^2_{Q_{\hat{a}\hat{a}}}} \geq c \tag{6}$$

where $\breve{a}_1$ and $\breve{a}_2$ represent the best and second-best ambiguity candidate, respectively; c is the threshold of R-ratio test, which is always larger than 1 and a larger value indicates higher reliability of the fixed solution. It can be set to 1.5–3.0 empirically (Han, 1997; Landau & Euler, 1992; Takasu & Yasuda, 2010), or calculated by controlling the failure rate (Teunissen & Verhagen, 2009). Different thresholds can produce different results, with too strict leading to frequent false-alarm errors and too loose leading to a large number of miss-detection errors.

In step (c), if the validation test fails, indicating potential unreliability, the float solution is then output. Otherwise, the fixed ambiguity vector is employed to update the float baseline solution:

$$\begin{aligned} \breve{b}(\breve{a}) &= \hat{b} - Q_{\hat{b}\hat{a}} Q_{\hat{a}\hat{a}}^{-1} (\hat{a} - \breve{a}) \\ Q_{\breve{b}(\breve{a})\breve{b}(\breve{a})} &= Q_{\hat{b}\hat{b}} - Q_{\hat{b}\hat{a}} Q_{\hat{a}\hat{a}}^{-1} Q_{\hat{a}\hat{b}} \end{aligned} \tag{7}$$

where $Q_{\hat{b}\hat{a}}$, $Q_{\hat{a}\hat{b}}$, and $Q_{\breve{b}(\breve{a})\breve{b}(\breve{a})}$ represent the VC matrix of $\hat{a}$, $\hat{b}$, and $\breve{b}(\breve{a})$, respectively.

Best integer equivariant estimation

ILS estimation includes both float and fixed solutions, depending on whether it passes the validation test. Nevertheless, it can be challenging to balance the false-alarm and miss-detection errors, which may

lead to a low accuracy of float solution or the severe bias of incorrectly fixed solution. In this case, the integer equivariant (IE) estimation can be another choice (Teunissen, 2003b). Firstly, considering an arbitrary linear function with two types of parameters, Eq. (1) can be rewritten as:

$$\theta = l_a^T a + l_b^T b \tag{8}$$

where l_a and l_b denote the coefficient matrices of a and b, respectively. Then, the BIE estimation of θ can be given as follows (Teunissen, 2003b):

$$\hat{\theta}_{BIE} = \frac{\sum_{z \in Z^n} \int_{R^p} (l_a^T z + l_b^T \beta) p_y(y + A(a-z) + B(b-\beta)) d\beta}{\sum_{z \in Z^n} \int_{R^p} p_y(y + A(a-z) + B(b-\beta)) d\beta} \tag{9}$$

where z and β denote the integer ambiguity candidate and baseline vector, respectively; $p_y(y)$ denotes the probability density function (PDF) of y, which is usually assumed to follow a Gaussian distribution with the PDF as follows:

$$p_y(y) = \frac{1}{(2\pi)^{\frac{m}{2}} \sqrt{\det Q_{yy}}} \\ \exp\left(-\frac{1}{2}\|y - Aa - Bb\|_{Q_{yy}}^2\right) \tag{10}$$

where m denotes the dimension of the observation vector; det and exp denote the determinant operator and exponential operation, respectively. Then, the BIE estimation of a and b in the Gaussian case can be simplifed as:

$$\hat{a}_{GBIE} = \sum_{z \in Z^n} z \frac{\exp(-\|\hat{a} - z\|_{Q_{\hat{a}\hat{a}}}^2 / 2)}{\sum_{z \in Z^n} \exp(-\|\hat{a} - z\|_{Q_{\hat{a}\hat{a}}}^2 / 2)} \\ = \sum_{z \in Z^n} z w_z^G(\hat{a}) \tag{11}$$

$$\hat{b}_{GBIE} = \hat{b} - Q_{\hat{b}\hat{a}} Q_{\hat{a}\hat{a}}^{-1}(\hat{a} - \hat{a}_{GBIE}) \tag{12}$$

where $w_z^G(\hat{a})$ denotes the weight factor of $\hat{a}$ for Gaussian BIE, with $\sum_{z \in Z^n} w_z^G(\hat{a}) = 1$. It can be found that the BIE estimator is essentially a weighted sum of all potential ambiguity candidates, and its weight depends on the PDF of GNSS observations.

BIE estimation based on Laplacian distribution

Compared with the ILS estimator, the BIE estimator exhibits some excellent properties, including the innecessity for the ambiguity reliability test, which reduces the risk of false-alarm and miss-detection errors. However, the BIE estimator is not always optimal in practical use, especially for urban environments with low-cost receivers, where GBIE poses an additional risk to AR. Therefore, this section delves into a detailed examination of the limitations of GBIE and explores the key issues associated with its alternative, LBIE.

Weight determination for candidates

The reasonable determination of the weight for candidates is the key to BIE estimator. As (11) shown, the weight factor of GBIE can be expressed as:

$$w_z^G(\hat{a}) = \frac{\exp(-\|\hat{a} - z\|_{Q_{\hat{a}\hat{a}}}^2 / 2)}{\sum_{z \in Z^n} \exp(-\|\hat{a} - z\|_{Q_{\hat{a}\hat{a}}}^2 / 2)} \leq 1 \tag{13}$$

Note that calculating the weight factor of GBIE involves two steps: first, perform an exponential operation on the quadratic form of residuals for each candidate, and then perform the normalization process. However, since the weight factor decreases exponentially, the weighting method may not always be effective, and a much lager weight may be assigned to the first best candidate once the quadratic form of residuals are excessively large. It implies that the performance of the BIE estimator at this point is similar to that of the ILS estimator, with an elevated risk of ambiguity misestimation, particularly when the stochastic model is inaccurate (Duong et al., 2021). We use a simple example based on a set of urban vehicular data to illustrate it. The data was collected by a low-cost receiver STA8100 of STMicroelectronics on June 26th, 2023. Additionally, the Least-squares Ambiguity Decorrelation Adjustment (LAMBDA) algorithm was adopted to output

Table 1 Weight factors and quadratic form comparison of Gaussian and Laplacian distributions

Order	Epoch 126,472 s with ILS Float			Epoch 126,530 s with ILS Fixed		
	Gaussian	Laplacian	$\|\hat{a} - z\|_{Q_{\hat{a}\hat{a}}}^2$	Gaussian	Laplacian	$\|\hat{a} - z\|_{Q_{\hat{a}\hat{a}}}^2$
1	0.993	0.264	363.837	1.000	0.741	41.237
2	0.007	0.248	373.886	0.000	0.107	200.863
…	…	…	…		…	…
9	0.000	0.038	717.505	0.000	0.010	558.537
10	0.000	0.036	732.136	0.000	0.010	562.145

Liu *et al. Satellite Navigation*   (2024) 5:12

Page 5 of 16

the estimated ambiguity candidates, with a limit of 500 for efficiency (Yang et al., 2024). Table 1 presents the weight factors of the first 10 candidates and their corresponding quadratic form of residuals. Two different epochs were compared, with one epoch outputting the float solution and the other epoch outputting the correctly fixed solution, respectively. The correctness of the fixed solution is validated against the reference truth provided by an integrated navigation system.

In the Gaussian case, the weight factor of the first candidate consistently dominates, exceeding 0.99, while the others are extremely small. It indicates that the AR performance of GBIE closely resembles that of the best integer candidate. When there is a significant difference between the best and second-best candidates (accepted by the validation test), the Gaussian weight is correct and results in the BIE solution that closely aligns with the ILS fixed solution (epoch 126,530 s). However, when the difference is not significant (rejected by the validation test), the ILS estimator produces a float solution, while the Gaussian weight of the first best candidate remains dominant (epoch 126,472 s). For example, the Gaussian weight drops sharply from 0.993 to 0.007, while the quadratic form of residuals only increases from 363.837 to 373.886. This indicates that the weight function of GBIE is too optimistic to maintain the reliability of BIE estimator. Therefore, we introduced the mathematically non-rigorous Laplacian distribution to address the issue of irrational allocation of Gaussian weight. If the GNSS observations y follow a Laplacian distribution, the PDF can be expressed as:

$$p_y(y) = \frac{1}{2\lambda\sqrt{\det Q_{yy}}} \exp\left(-\frac{\sqrt{||y - Aa - Bb||^2_{Q_{yy}}}}{\lambda}\right) \quad (14)$$

where λ is a scaling factor, an empirical threshold that can be set to 4 (Vollath & Talbot, 2013), and will be analyzed in the following. Similar to GBIE, the BIE estimation of a and b in the Laplacian case can be simplified as:

$$\hat{a}_{LBIE} = \sum_{z \in Z^n} z w_z^L(\hat{a}) \quad (15)$$

$$\hat{b}_{LBIE} = \hat{b} - Q_{\hat{b}\hat{a}} Q_{\hat{a}\hat{a}}^{-1}(\hat{a} - \hat{a}_{LBIE}) \quad (16)$$

$$w_z^L(\hat{a}) = \frac{\exp(-\sqrt{||\hat{a} - z||^2_{Q_{\hat{a}\hat{a}}}}/\lambda)}{\sum_{z \in Z^n} \exp(-\sqrt{||\hat{a} - z||^2_{Q_{\hat{a}\hat{a}}}}/\lambda)} \quad (17)$$

where $w_z^L(\hat{a})$ denotes the weight factor of $\hat{a}$ for Laplacian BIE, with $\sum_{z \in Z^n} w_z^L(\hat{a}) = 1$. It can be found that unlike GBIE, LBIE assigns more weight to other candidates by applying a square root operation to the quadratic form
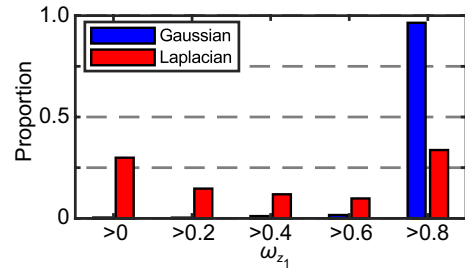

Fig. 1 Weight distribution of the best ambiguity candidate for Gaussian and Laplacian distributions

of residuals and multiplying it by a scaling factor. And it is an effective way to prevent incorrectly fixed solution and increase reliability, even if the accuracy may be lost somewhat when the success rate of ILS is high, as the correct best candidate may be contaminated through the weighted fusion. Figure 1 shows the distribution of the weight factors of the best candidate for all epochs (nearly 3000 s) in this set of data, with blue and red bars representing Gaussian distribution and Laplacian distribution, respectively. The processing strategy is the same as before. A higher weight factor indicates a stronger influence of the best candidate on the weighted fusion. It can be found that in the Gaussian case the weight of the best candidate consistently dominates, while the Laplacian case assigns less weight, providing additional reliability. In conclusion, we recommend using the more reliable Laplacian distribution to determine the weights for candidates, particularly when the quadratic form of ambiguity residuals are excessively large, possibly due to the deficiencies in the stochastic model.

To further validate the distribution characteristics of GNSS observations using real-measured data, we analyzed the differences between float and fixed ambiguity solutions, defined as ambiguity residuals. The data remains consistent with the one described earlier. Additionally, the float solution is obtained from the KF, and the fixed solution is estimated using the ILS estimation, implemented by the LAMBDA algorithm with an R-ratio test of threshold 2.5. The correctness of the fixed solution is validated against the reference truth provided by an integrated navigation system. Assuming that the GNSS observations follow a Gaussian distribution, the ambiguity residuals can be expressed as Duong et al. (2021):

$$\Delta a = \hat{a} - \breve{a} \sim N(0, Q_{\hat{a}\hat{a}}) \quad (18)$$

Due to the presence of reference satellites, the ambiguity parameters are highly correlated, resulting in a fully populated VC matrix. Therefore, Cholesky
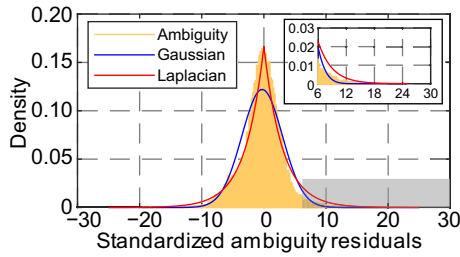
Liu *et al. Satellite Navigation*   (2024) 5:12

Page 6 of 16

Fig. 2 Frequency distribution histogram of standardized ambiguity residuals and the PDFs of Gaussian and Laplacian distributions. The zoom-in window depicts the details about the gray shaded area

factorization is adopted to normalize Δa in the following process:

$$Q_{\hat{a}\hat{a}} = LL^T \tag{19}$$

$$\Delta \bar{a} = L^{-1}\Delta a \sim N(0, I_m) \tag{20}$$

where $\Delta \bar{a}$ denotes the standardized ambiguity residuals, and I_m denotes the m-dimensional identity matrix. Then, the frequency distribution histogram of standardized ambiguity residuals and the PDFs of the two distributions are plotted in Fig. 2. The MATLAB toolbox "Distribution Fitter" is employed to generate the best fit of the Gaussian distribution, represented by the blue solid line in the figure. The red solid line represents the Laplacian distribution with a scaling factor of 3. It can be found that the Laplacian distribution provides a better fit than the Gaussian distribution. Note that the scaling factor is closely related to the characteristics of GNSS receivers and observation environments and needs to be finely processed.

Number determination of candidates

Another key issue in the application of BIE is determining the number of ambiguity candidates to be included. Due to the impossibility in obtaining a theoretical estimation of BIE using infinite sets of candidates in space Z^n, approximation processing is required. Fortunately, the weight for candidates follows an exponential form and rapidly decays as the distance between the integer candidate and the float solution increases. Consequently, various methods have been successively proposed to limit the number of candidates, including the fixed threshold test, central Chi-squared test based on a given significance level (Teunissen, 2005b), weight ratio test in the iFlex method (Vollath & Talbot, 2013), OIA test (Ma et al., 2022), and an unsupervised machine learning strategy (Zhang et al., 2023a).

Among them, the fixed threshold test is not sensitive to the data and faces the challenges in balancing performance and efficiency. The central Chi-square test suffers from model distortion issues, leading to poor stability in practical use. The latter two methods evaluate the weight factor of the latest included candidate and do not stop the selection until its weight factor is significantly smaller than the best candidate or the total weight of all candidates included. The unsupervised machine learning strategy uses the K-means++ algorithm to select candidates, involving an iterative process. Considering both efficiency and performance, we utilize the OIA test for number determination of candidates and discuss the distinctions between the iFlex test and OIA test.

The basic idea of the iFlex test is to include those candidates that exhibit no substantial difference in the weight factor compared to the best candidate. The level of differentiation is determined by applying an empirical threshold, expressed as follows:

$$\frac{w_{z_j}(\hat{a})}{w_{z_1}(\hat{a})} \leq \gamma_1 \tag{21}$$

where $w_{z_1}(\hat{a})$ is the weight factor of the first best candidate, and $w_{z_j}(\hat{a})$ is the weight factor of the jth candidate. As the candidates output by the LAMBDA algorithm are sorted according to the quadratic form of ambiguity residuals, this equation implies that the weight factor of the discarded candidates is at least γ_1 times smaller than the weight factor of the best candidate. The smaller the value of γ_1, the more candidates are included in the BIE estimator. Typically, it can be set to 0.01 (Vollath & Talbot, 2013), at which point the discarded candidates have little impact on the final BIE solution. Subsequently, introducing (13) and (17) into (21) provides the formula to select candidates for Gaussian distribution and Laplacian distribution, respectively:

$$||\hat{a} - z_j||^2_{Q_{\hat{a}\hat{a}}} \geq ||\hat{a} - z_1||^2_{Q_{\hat{a}\hat{a}}} - 2\ln(\gamma_1) \tag{22}$$

$$||\hat{a} - z_j||^2_{Q_{\hat{a}\hat{a}}} \geq [\sqrt{||\hat{a} - z_1||^2_{Q_{\hat{a}\hat{a}}}} - \lambda \ln(\gamma_1)]^2 \tag{23}$$

where z_j is the latest included candidate with the largest quadratic form of residuals. Teunissen (2005a) first defined the OIA estimator as the one with the largest possible success rate under a given fail-rate. Later, the OIA test was employed for ambiguity validation in Wu and Bian (2015), and Ma et al. (2022) expanded its application to determine the number of candidates in BIE. The OIA test criterion for GBIE can be expressed as follows:

$$\frac{w_{z_j}^G(\hat{a})}{\sum\limits_{i=1}^{j} w_{z_i}^G(\hat{a})} = \frac{\exp\left(-||\hat{a}-z_j||_{Q_{\hat{a}\hat{a}}}^2 \big/ 2\right)}{\sum\limits_{i=1}^{j} \exp\left(-||\hat{a}-z_i||_{Q_{\hat{a}\hat{a}}}^2 \big/ 2\right)} \leq \gamma_2 \quad (24)$$

where γ_2 is a test threshold, which can be set to 0.01 concerning γ_1 in the iFlex test. It can be found that the OIA test converges faster with the increase of the quadratic form of residuals, compared to the iFlex test, as the denominator is the sum of the weight of all the candidates. Similarly, the OIA test criterion for LBIE can be derived as:

$$\frac{w_{z_j}^L(\hat{a})}{\sum\limits_{i=1}^{j} w_{z_i}^L(\hat{a})} = \frac{\exp\left(-||\hat{a}-z_j||_{Q_{\hat{a}\hat{a}}} \big/ \lambda\right)}{\sum\limits_{i=1}^{j} \exp\left(-||\hat{a}-z_i||_{Q_{\hat{a}\hat{a}}} \big/ \lambda\right)} \leq \gamma_2 \quad (25)$$

To further compare the performances of the two methods, we analyze the numerical characteristics of the BIE solutions derived from a different number of candidates. In the analysis, we use the LBIE estimator, employing the same data and processing strategy as before. Three different methods are compared, including the fixed threshold test, iFlex test, and OIA test. Figure 3 shows the differences between the float solutions, integer candidates determined by different methods, BIE solutions, and their "true values". Additionally, the blue circle represents the float solutions, the red triangle represents the BIE solutions, and the yellow star represents the integer candidates. For display purposes, we set the best candidate as the true value, coinciding with the horizontal axis. The remaining candidates fluctuate on both sides of the horizontal axis, with a maximum deviation close to 9 cycles, indicating the poor accuracy of float solution. It can be found that the number of candidates determined by the OIA test is only 27, significantly lower than the fixed threshold test of 500 and the iFlex test of 110. Furthermore, the difference between different BIE solutions is insignificant, which essentially coincide with the best candidate. It suggests that only a few candidates play a dominant role in the BIE estimator, and the OIA test

adopted in this paper effectively controls the number of candidates involved.

Reliability evaluation of BIE solution

In the past few years, many GNSS applications emerged in urban environments, so the measure of trust in the correctness of the navigation information is receiving an increasing attention. It is essentially a problem of GNSS integrity in urban environments, but unfortunately, there are no mature methods that can be implemented by urban GNSS receivers alone (Zhu et al., 2018). The ILS estimation partially addresses the concept of integrity by distinguishing between float and fixed solutions through ambiguity validation. Once the ambiguities are successfully fixed, the accuracy of baseline can reach the centimeter level, leading GNSS users to place trust in the fixed solution and demand a higher fixed rate. However, for BIE estimation, while it mitigates the risk of incorrectly fixing and bias due to unfixed solution, the indiscriminate output of results poses a significant challenge to the further application of the provided information. Therefore, the evaluation of BIE solution is of great necessity. Yu et al. (2021) derived the VC matrix of GBIE estimator and proposed a criterion for determining reliability. This section further derives the VC matrix of LBIE estimator and applies it to the reliability evaluation of BIE solution.

Assuming that the number of ambiguity candidates t used for the weighted fusion of LBIE estimator has been determined by the OIA test according to (25), (15) can be rewritten as:

$$\hat{a}_{LBIE} = \sum_{i=1}^{t} z_i w_{z_i}^L(\hat{a}) \quad (26)$$

Then, differentiating (26) yields the following formula:

$$d\hat{a}_{LBIE} = \sum_{i=1}^{t} dw_{z_i}^L(\hat{a}) z_i = \sum_{i=1}^{t} z_i \frac{\partial w_{z_i}^L(\hat{a})}{\partial \hat{a}^T} d\hat{a} \quad (27)$$
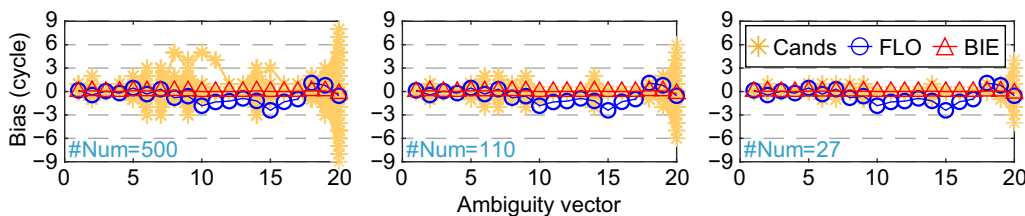
with:

Fig. 3 Differences between the integer candidates and their true values, from left to right are fixed threshold (500), iFlex test, and OIA test

$$\frac{\partial w_{z_i}^L(\hat{a})}{\partial \hat{a}^T} = \frac{\frac{\partial T_i}{\partial \hat{a}^T}\sum_{j=1}^t T_j - T_i \sum_{j=1}^t \frac{\partial T_j}{\partial \hat{a}^T}}{\left[\sum_{j=1}^t T_j\right]^2} \quad (28)$$

where $T_j = \exp(-||\hat{a} - z_j||_{Q_{\hat{a}\hat{a}}} / \lambda)$. Further differentiation can be performed to derive $\partial T_j / \partial \hat{a}^T$ as:

$$\begin{aligned}\frac{\partial T_j}{\partial \hat{a}^T} &= \frac{\partial \exp\left(-||\hat{a} - z_j||_{Q_{\hat{a}\hat{a}}} / \lambda\right)}{\partial \hat{a}^T} \\ &= -\frac{1}{\lambda} T_j \frac{\partial ||\hat{a} - z_j||_{Q_{\hat{a}\hat{a}}}}{\partial \hat{a}^T} \\ &= -\frac{T_j}{\lambda ||\hat{a} - z_j||_{Q_{\hat{a}\hat{a}}}} (\hat{a} - z_j)^T Q_{\hat{a}\hat{a}}^{-1}\end{aligned} \quad (29)$$

Substituting (29) into (28), we can obtain the following formula:

$$\begin{aligned}\frac{\partial w_{z_i}^L(\hat{a})}{\partial \hat{a}^T} &= \frac{\frac{\partial T_i}{\partial \hat{a}^T}\sum_{j=1}^t T_j - T_i \sum_{j=1}^t \frac{\partial T_j}{\partial \hat{a}^T}}{\left[\sum_{j=1}^t T_j\right]^2} \\ &= \frac{-\frac{T_i}{\lambda ||\hat{a} - z_i||_{Q_{\hat{a}\hat{a}}}}(\hat{a} - z_i)^T Q_{\hat{a}\hat{a}}^{-1}\sum_{j=1}^t T_j - T_i \sum_{j=1}^t -\frac{T_j}{\lambda ||\hat{a} - z_j||_{Q_{\hat{a}\hat{a}}}}(\hat{a} - z_j)^T Q_{\hat{a}\hat{a}}^{-1}}{\left[\sum_{j=1}^t T_j\right]^2} \\ &= \frac{\sum_{j=1}^t \frac{T_j}{||\hat{a} - z_j||_{Q_{\hat{a}\hat{a}}}}(\hat{a} - z_j)^T - \frac{1}{||\hat{a} - z_i||_{Q_{\hat{a}\hat{a}}}}(\hat{a} - z_i)^T \sum_{j=1}^t T_j}{\lambda \left[\sum_{j=1}^t T_j\right]^2} T_i Q_{\hat{a}\hat{a}}^{-1}\end{aligned} \quad (30)$$

Thus, we can calculate the VC matrix of $\hat{a}_{LBIE}$ by applying the law of error propagation:

$$Q_{\hat{a}_{LBIE}\hat{a}_{LBIE}} = \sum_{i=1}^t z_i \frac{\partial w_{z_i}^L(\hat{a})}{\partial \hat{a}^T} Q_{\hat{a}\hat{a}} \sum_{i=1}^t \frac{\partial w_{z_i}^L(\hat{a})}{\partial \hat{a}} z_i^T \quad (31)$$

Then, $Q_{\hat{b}_{LBIE}\hat{b}_{LBIE}}$ is also calculated according to (15), similar to the Gaussian case, which is illustrated clearly in Yu et al. (2021):

$$Q_{\hat{b}_{LBIE}\hat{b}_{LBIE}} = KQ_{\hat{a}\hat{a}}K^T + Q_{\hat{b}\hat{a}}K^T + KQ_{\hat{a}\hat{b}} + Q_{\hat{b}\hat{b}} \quad (32)$$

with:

$$K = -Q_{\hat{b}\hat{a}}Q_{\hat{a}\hat{a}}^{-1}\left(E - \sum_{i=1}^t z_i \frac{\partial w_{z_i}^L(\hat{a})}{\partial \hat{a}^T}\right) \quad (33)$$

Finally, the trace of the VC matrix can serve as an indicator of reliability evaluation, following the criterion:

$$trac(Q_{\hat{b}_{LBIE}\hat{b}_{LBIE}}) < trac(Q_{\hat{b}\hat{b}}) \quad (34)$$

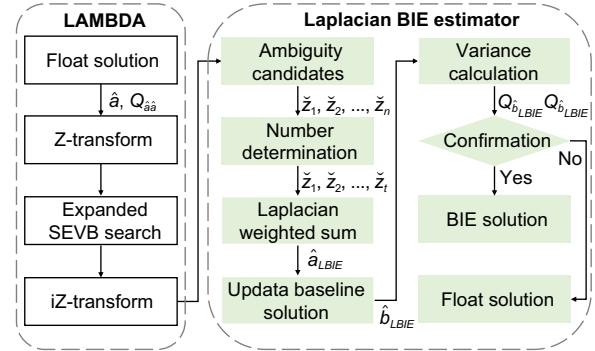It implies that the BIE solution is accepted as the output only when its accuracy surpasses that of the float

Fig. 4 Flowchart of the improved BIE estimation method

solution. This criterion stems from the practical scenario where the accuracy of the BIE solution may not always be optimal if the float ambiguity solution is biased due to the significant unmodeled errors. Based on the aforementioned analysis, the algorithm flowchart of the proposed improved BIE estimation method in this paper is depicted in Fig. 4. Initially, the float solution is estimated through the KF model with velocity constraint, followed by a Z-transformed decorrelation to reconstruct the float ambiguities and its VC matrix according to the LAMBDA algorithm; next, the ambiguity candidates are searched, and the included candidates are determined by the OIA test according to (25); subsequently, the included

Table 2 Common processing strategies of ILS-PAR, GBIE, TBIE, and LBIE solutions

Items	Strategies
Constellations and frequencies	GPS (L1 + L5)/Galileo (E1 + E5a)/BDS (B1I + B2a)
Ephemeris	Broadcast ephemeris
Cut-off elevation	15°
Cut-off C/N0	25dB-Hz
Weighting function	C/N0-dependent weighting function
Ambiguities	Multi-epoch solution
σ_P^2 / σ_L^2	$(300 : 1)^2$

Liu *et al. Satellite Navigation*　　(2024) 5:12

Page 9 of 16

Table 3 Detailed experimental information of the two tests

	Test 1	Test 2
Experimental time	November 14, 2021	June 26, 2023
Rover station	Engineering prototype of Huawei Mate40 smartphone	STMicroelectronics STA8100 single-chip GNSS receiver
Reference station	Trimble Alloy with UniStrong UA91 3D choke-ring antenna	FindCM service from Qianxun Spatial Intelligence Inc
Baseline length	< 20 km	< 5 km
Data duration	10 min	1 h
Simpling interval	1 s	

candidates are used to calculate the BIE solution through a weighted sum, whose weight factors are determined using (17); finally, the VC matrix of the BIE solution is computed to perform the reliability evaluation.

Field test results and discussions

Experiment description

The algorithm implementation is based on the GNSS dynamic positioning software (KinPOS V3.0) developed by the School of Geodesy and Geomatics at Wuhan University. The parameter settings and processing strategies are outlined in Table 2. Four different estimation methods are compared, i.e., (a) ILS fixed solution realized by the LAMBDA algorithm with a PAR strategy based on carrier-to-noise ratio (CNR), where the iteration continues until passing the R-ratio test with a threshold of 2.5 or the remaining ambiguities falling below 6 (hereinafter referred to as ILS-PAR); (b) the traditional GBIE with the iFlex test, where γ_1 is set to 0.01 (hereinafter referred to as GBIE); (c) BIE estimation using multivariate t-distribution with 3 degrees of freedom, where Euclidean norm of coordinates' corrections is used to select candidates (Duong et al., 2021, hereinafter referred to as TBIE); (d) the proposed LBIE with the OIA test, where γ_2 is set to 0.01 (hereinafter referred to as LBIE). For the BIE estimation, an upper limit of 500 is applied to prevent over-searching of ambiguity candidates.

As shown in Table 3, two typical vehicular experiments in urban environments were performed for evaluation of performance. The first experiment was conducted on the Gaoxin Avenue in Wuhan City, with a relatively open observation environment (hereinafter referred to as test 1). Here the engineering prototype of Huawei Mate40 smartphone was used and placed on the top of the vehicle. The trajectory and equipment installation of the experiment are depicted in Fig. 5. The second experiment was conducted in the High-tech Zone of Chengdu City with complex observation environments, i.e., tunnels, viaducts, buildings, and trees, which is a typical urban environment (hereinafter referred to as test 2). For this test, a low-cost GNSS receiver, STA8100
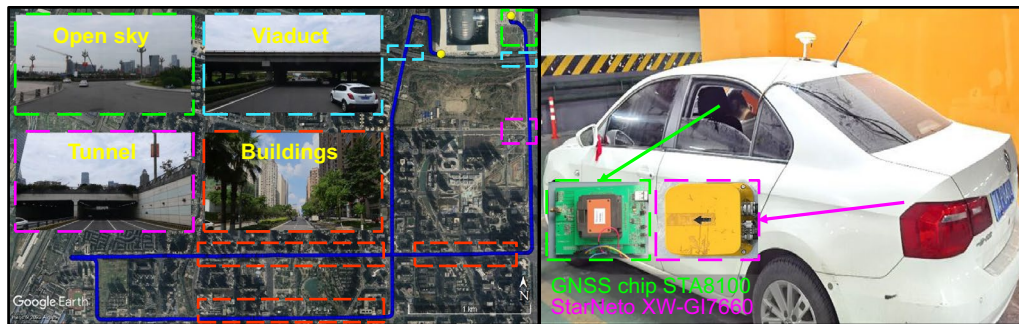

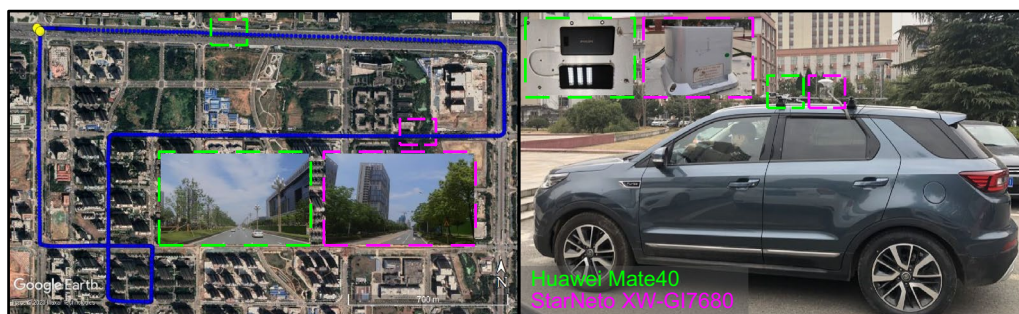**Fig. 6** Trajectory (left) and equipment setup (right) in test 2

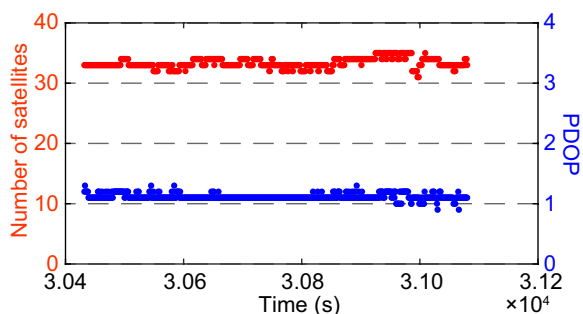**Fig. 5** Trajectory (left) and equipment setup (right) in test 1

Liu *et al. Satellite Navigation*   (2024) 5:12

Page 10 of 16

Fig. 7 Number of satellites (red point) and PDOP values (blue point) in test 1

Table 4 Statistics of pseudorange DD and carrier phase TD residuals in test 1

		Phase TD (%)			Code DD RMS (m)
		> 1 cycle	> 5 cycle	> 10 cycle	
GPS	L1	8.50	0.30	0.00	8.133
	L5	17.39	0.00	0.00	0.595
GAL	E1	0.80	0.00	0.00	3.974
	E5a	6.58	0.00	0.00	0.540
BDS	B1I	29.41	11.29	3.31	5.538
	B2a	18.23	6.17	1.10	0.793

from STMicroelectronics, was used, and the trajectory and equipment installation are depicted in Fig. 6. Additionally, in all tests, the StarNeto XW-GI7680 and XW-GI7660 integrated navigation systems were used to provide references, which was processed by IE software. To analyze the quality of GNSS observations in urban environments, the DD and triple-difference (TD) combinations are used to extract the residuals of pseudorange and carrier phase, respectively (Tao et al., 2023).

Performance in the urban expressway for smartphone

Figure 7 depicts the number of visible satellites and position dilution of precision (PDOP) values in test 1. It can be found that the number of satellites exceeds 30, with fluctuations of 2–3 over time, and the PDOP values consistently remain within 2, indicating a good quality of observations. The comparison of pseudorange DD residuals and carrier phase TD residuals for the smartphone are also depicted in Fig. 8 and Table 4, respectively. Even in the open conditions, the pseudorange noise of L1, E1, and B1I of smartphones are 8.133 m, 3.974 m, and 5.538 m, with a discernible abnormal probability distribution. Remarkably, the pseudorange accuracy of the L5 band surpasses the L1 band, presenting opportunities for the applications of high-precision kinematic positioning algorithms on smartphones (Miao et al., 2022). Additionally, BDS B1I and B2a exhibit the highest proportion of carrier phase noise, exceeding 20% and 30% for more than 1 cycle, while GALILEO E1 and E5a display the smallest carrier phase noise.

As depicted in Fig. 9, in the urban expressway test for the smartphone, the ILS-PAR method only fixes the ambiguity successfully in a few epochs and yields limited improvement compared to the float solution. Similarly, the successful estimation rate of GBIE is only 14.77% for the computer truncation error generated by the direct exponential operation on the quadratic form of ambiguity residuals. Contrastingly, the TBIE and LBIE solutions have similar positioning errors of less than 0.5 m in east (*E*), north (*N*), and up (*U*) directions, and obtain more than 50% improvements compared to other methods. The idea of assigning more weight to other candidates indeed improves the AR performance of smartphone positioning in kinematic urban environments. Note that there are also some discontinuous jump points in the positioning error sequence of LBIE solution, which can be attributed to two main factors: firstly, the failure of the variance reliability test leads to the output of the float solution; secondly, the LBIE solution also encounters occasional ambiguity estimation errors, albeit with a lower probability of occurrence.

Performance in the urban canyon for STA8100

As depicted in Fig. 10, in open-sky conditions, the visibility of satellites hovers around 30, but it fluctuates greatly and sometimes even drops below 10 in urban-canyon conditions. The frequent changes in the observation environment lead to a varying geometric distribution of satellites and discontinuity of carrier phase observations, which poses great challenges to AR. Figure 11 and Table 5
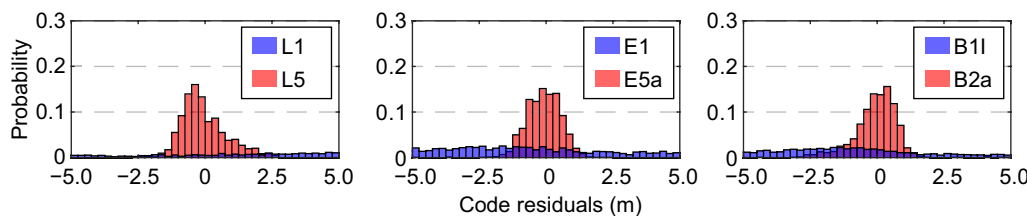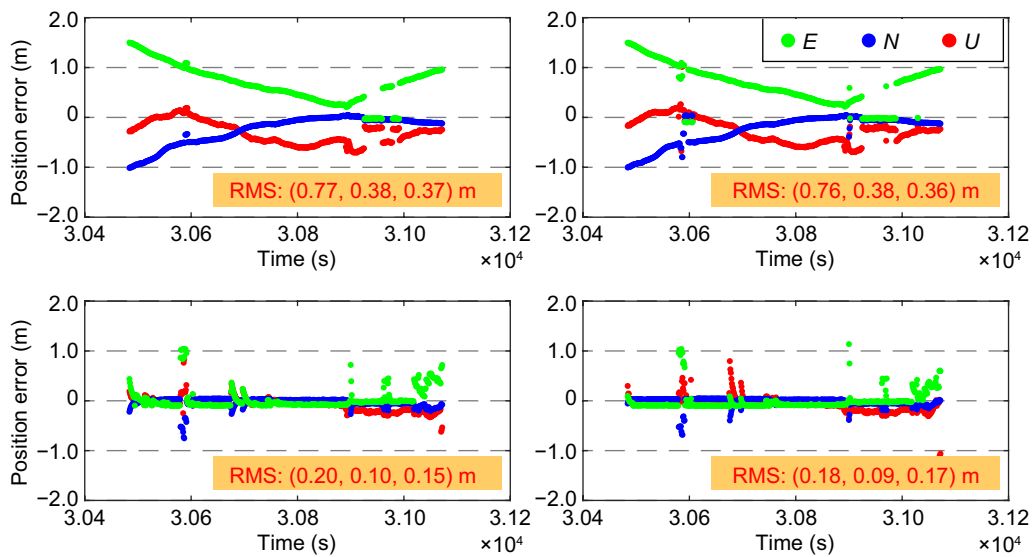

Fig. 8 Pseudorange DD residuals in test 1

Fig. 9 Positioning errors of ILS-PAR (top left), GBIE (top right), TBIE (bottom left), and LBIE (bottom right) solutions in test 1
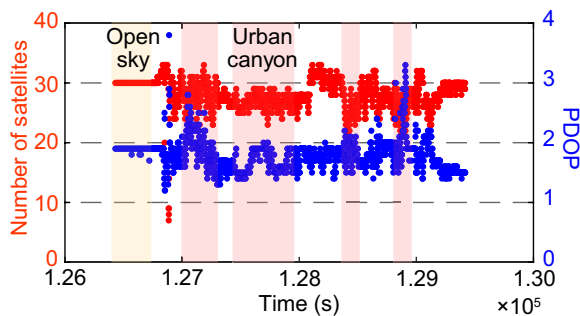

Fig. 10 Number of satellites (red point) and PDOP values (blue point) in test 2

present a comparison of pseudorange DD residuals and carrier phase TD residuals for multi-GNSS observations with STA8100, respectively. Notably, in the urban-canyon test, the pseudorange accuracy of L1, E1, and B1I is poor, with root mean square (RMS) values of approximately 5.357 m, 4.195 m, and 3.820 m, respectively, nearly twice that of L5, E5a, and B2a. This aligns with the design

concept of the L5 band. Additionally, carrier phase noise accounts for nearly 15% for more than 1 cycle and 10% for more than 10 cycles, except for E5a. The B2a exhibits the largest percentage of 28.47% for more than 1 cycle, indicating frequent cycle jumps in carrier phase observations and significantly impacting the accurate fixation of ambiguities.

The positioning errors of four different methods in open-sky conditions (epoch 126,431 s to 126,846 s) are depicted in Fig. 12, with RMS values highlighted in red. The green, blue, and red lines are for the *E*, *N*, and **U** directions, respectively. In open-sky conditions, the float ambiguities can be easily resolved, and all methods demonstrate high positioning accuracy, with TBIE and LBIE showing slight improvement. In addition, due to the dominant weight factor of the best candidate in the weighted fusion, the GBIE solution follows a similar error sequence trend to that of the ILS-PAR.

Figure 13 further depicts the positioning errors of four different methods in typical urban-canyon conditions (epoch 127,445 s to 127,969 s), where roads are surrounded by tall buildings and dense trees. It is evident
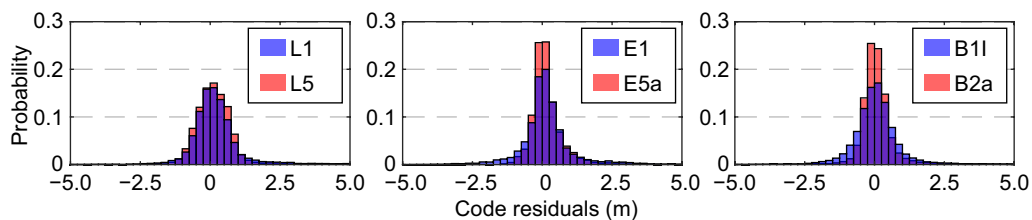

Fig. 11 Pseudorange DD residuals in test 2

Liu *et al. Satellite Navigation* (2024) 5:12

Page 12 of 16

Table 5 Statistics of pseudorange DD and phase TD residuals in test 2

		Phase TD (%)			Code DD RMS (m)
		> 1 cycle	> 5 cycle	> 10 cycle	
GPS	L1	18.01	15.10	12.76	5.357
	L5	17.62	14.83	13.23	2.506
GAL	E1	18.87	15.75	13.88	4.195
	E5a	5.98	3.45	2.83	2.967
BDS	B1I	20.25	16.89	14.87	3.820
	B2a	28.47	24.93	23.65	2.155

that the float solution maintains a high level of accuracy, within 1 m. However, due to frequent occurrace of gross errors and cycle slips, the ILS-PAR estimator still struggles to fix ambiguity. Notably, the GBIE solution exhibits two situations attributed to the large quadratic form of ambiguity residuals. On the one hand, at successful GBIE epochs, the weight factor of the best candidate approaches 1, resulting in positioning accuracy similar to that of the correctly fixed solution. This helps mitigate false-alarm errors caused by unreasonable setting of the R-ratio test threshold compared to the ILS-PAR. On the other hand, due to the direct exponential operation on the residual quadratic form, the weight factor of the best candidate may be zero, resulting in GBIE estimation failure and the output of a float solution with poor accuracy. Conversely, the LBIE solution addresses the accuracy layering issue between the float and fixed solutions through weighted fusion and avoids estimation failure. It achieves accuracy of 0.03 m, 0.05 m, and 0.16 m in *E*, *N*, and *U*

directions, respectively, surpassing the performance of ILS-PAR and GBIE methods, and comparable to that of the TBIE method.

Figure 14 depicts the cumulative distribution function (CDF) of the positioning errors for all epochs, which can lead to similar conclusions. The TBIE and LBIE solutions demonstrate significant superiority, while GBIE slightly outperforms ILS-PAR. Specifically, the proportion of positioning errors less than 1.0 m is 97.85%, 98.25%, 97.85, and 98.12% for ILS-PAR, GBIE, TBIE, and LBIE, respectively. In the zoom-in window, the proportion of positioning errors within 0.1 m is approximately 55.42% and 60.30% for ILS-PAR and GBIE. Meanwhile, TBIE and LBIE achieve 82.41% and 81.65%, representing an improvement of over 20%. Summarizing the statistical results for all epochs in Table 6, the positioning accuracy of LBIE in *E*, *N*, and *U* directions is 0.112 m, 0.107 m, and 0.252 m, respectively, slightly better than TBIE and much better than GBIE and ILS-PAR. Specifically, it exhibits improvements of 17.6%, 27.2%, and 26.1% over GBIE, and 23.3%, 28.2%, and 30.6% over ILS-PAR, respectively, which reflects the significant reliability of BIE estimation with heavy-tailed distributions.

Analysis of time consumption

To evaluate the efficiency of the four different methods, the time consumption of the entire RTK positioning process was calculated. The computations were executed in Visual Studio 2019 on a computer equipped with a 12th Gen Intel (R) Core (TM) i7-12700 K 3.60 GHz processor running Windows 10 64-bit Professional. As shown in Fig. 15 and summarized in Table 7,
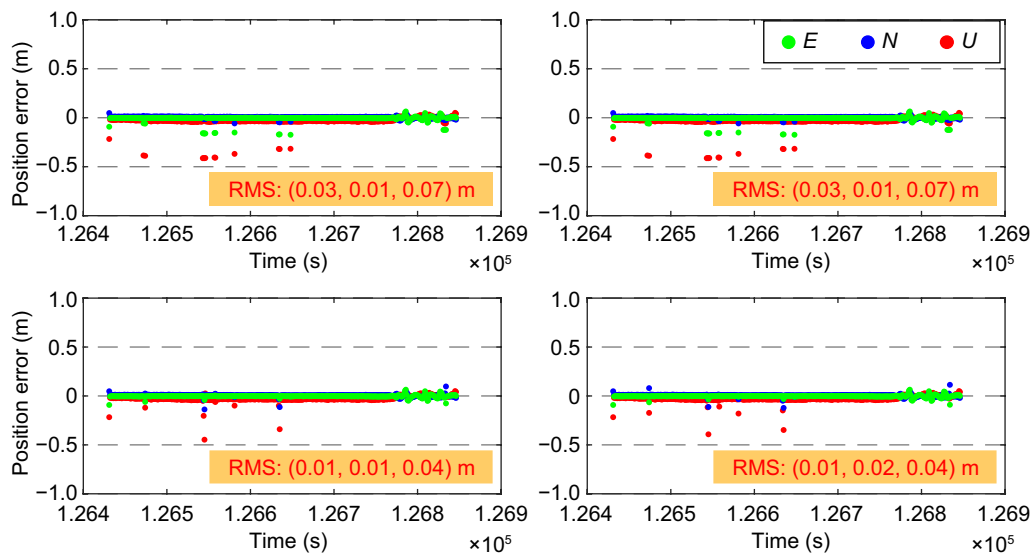

Fig. 12 Positioning errors of ILS-PAR (top left), GBIE (top right), TBIE (bottom left), and LBIE (bottom right) solutions in open-sky conditions in test 2
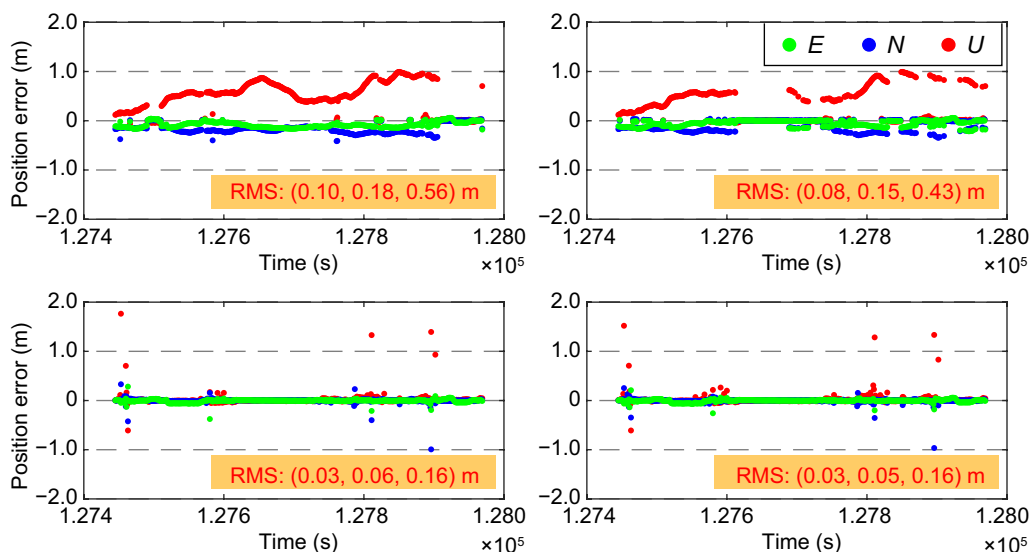
Fig. 13 Positioning errors of ILS-PAR (top left), GBIE (top right), TBIE (bottom left), and LBIE (bottom right) solutions in urban-canyon conditions in test 2
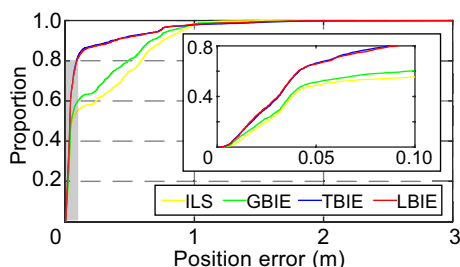

Fig. 14 Cumulative distribution function of three-dimensional positioning errors in ILS-PAR, GBIE, TBIE, and LBIE solutions. The zoom-in window depicts the details about the gray shaded area

Table 6 Statistics of RMS of positioning errors in ILS-PAR, GBIE, TBIE, and LBIE solutions

Method	E (m)	N (m)	U (m)
ILS-PAR	0.146	0.149	0.363
GBIE	0.136	0.147	0.341
TBIE	0.116	0.111	0.261
LBIE	0.112	0.107	0.252

ILS-PAR involves exactly 2 candidates to perform the R-ratio test. For GBIE, due to the rapid decrease in the weight factors during the weighted process, the average number of candidates is approximately 2, with test values of 1.77 and 2.42, respectively, posing a significant risk of wrong fixing of ambiguities. However, TBIE and LBIE address it better by spreading out the weights to other candidates, with the former averaging over 60 candidates and the latter over 10. As for the efficiency shown in Fig. 16 and Table 7, there is marginal difference between GBIE and LBIE, with both increasing by approximately 30–40% compared to ILS-PAR. It is primarily because the main part of the computational time in AR is the search process for ambiguity candidates, and both BIE methods have the same pre-searching number of 500, while the number for ILS-PAR is only 2. It is worth noting that the computational time using TBIE is approximately twice that of using LBIE, as it involves the process of calculating the updated coordinate vector for each integer candidate.

Conclusions

Compared to the float and fixed solutions, the BIE estimator considers almost all integer candidates of ambiguity, aligning with the concept of full probability estimation and proving more suitable for urban environments. This paper introduces an improved BIE estimation method with Laplacian distribution to enhance the performance of urban low-cost positioning. Firstly, the Laplacian distribution is incorporated into the weighting function of BIE to address the issue of irrational weight allocation associated with Gaussian distribution. Additionally, a criterion based on the OIA test is employed to determine
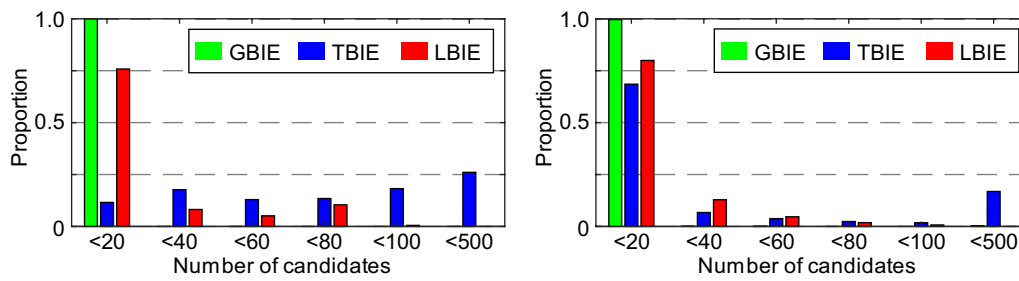
Liu *et al. Satellite Navigation*   (2024) 5:12

Page 14 of 16

Fig. 15 Number of ambiguity candidates in GBIE, TBIE, and LBIE solutions in test 1 (left) and test 2 (right)

Table 7 Average number of ambiguity candidates and time consumption in ILS-PAR, GBIE, TBIE, and LBIE solutions

Method	Average candidates		Average time (ms)	
	Test 1	Test 2	Test 1	Test 2
ILS-PAR	2.00	2.00	5.01	8.19
GBIE	1.77	2.42	6.68	10.76
TBIE	64.98	61.69	13.18	23.90
LBIE	16.73	11.51	7.09	10.61

the number of candidates. Finally, the VC matrix of the LBIE solution is derived to evaluate its reliability.

Two typical vehicular experiments in urban environments were conducted to evaluate the performance of the proposed BIE estimation by using the Huawei Mate40 smartphone and STMicroelectronics low-cost receiver STA8100, respectively. Four different methods are compared, i.e., ILS-PAR, GBIE, TBIE, and LBIE. The results show that the proposed LBIE method has similar positioning accuracy to TBIE and significantly outperforms the ILS-PAR and GBIE methods by spreading out the weights to other candidates. For the urban expressway test with the smartphone, the LBIE method has

positioning errors of less than 0.5 m in three directions and obtain more than 50% improvements compared to the ILS-PAR and GBIE methods. For the urban canyon test with the STA8100 receiver, the positioning accuracy of LBIE in three directions is 0.112 m, 0.107 m, and 0.252 m, respectively, with improvements of 17.6%, 27.2%, and 26.1% compared to GBIE, and 23.3%, 28.2%, and 30.6% compared to ILS-PAR. Moreover, its computational time increases by 30%-40% compared to ILS-PAR and is approximately half of that using TBIE.

In summary, the proposed LBIE method significantly improved positioning accuracy and reliability, effectively addressing the challenges of AR in urban low-cost RTK positioning. Due to space limitations, the thresholds used were not discussed in detail, especially the scaling factor of the Laplacian distribution. Future research should explore adaptive adjustments of the thresholds for different scenarios, enhancing the universality of strategies. Additionally, other sensors, such as inertial measurement units, can be introduced into urban vehicular RTK positioning to provide continuous and accurate positioning and navigation services, further enhancing GNSS integrity monitoring of vehicle positioning in urban environments.
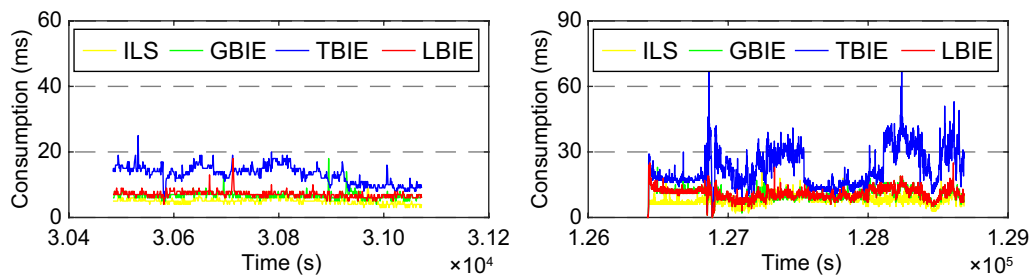

Fig. 16 Time consumption for a single epoch in ILS-PAR, GBIE, TBIE, and LBIE solutions in test 1 (left) and test 2 (right)

Liu *et al. Satellite Navigation*   (2024) 5:12

Page 15 of 16

Abbreviations

AR	Ambiguity resolution
BIE	Best integer equivariant
CDF	Cumulative distribution function
CNR	Carrier-to-noise ratio
DD	Double-difference
E	East
GBIE	Gaussian best integer equivariant
GNSS	Global navigation satellite system
IA	Integer aperture
IAR	Integer ambiguity resolution
IE	Integer equivariant
ILS	Integer least squares
KF	Kalman filter
LAMBDA	Least-squares ambiguity decorrelation adjustment
LBIE	Laplacian best integer equivariant
LS	Least squares
MMSE	Minimum mean squared error
N	North
NLOS	Non-line-of-sight
OIA	Optimal integer aperture
PAR	Partial ambiguity resolution
PDF	Probability density function
PDOP	Position dilution of precision
PNT	Navigation, positioning, and timing
PPP	Precision point positioning
RMS	Root mean square
RTK	Real-time kinematic
TBIE	T-distribution best integer equivariant
TD	Triple-difference
U	Up
VC	Variance-covariance

Author contributions
WK.L. and XH.Z. provided the initial idea and designed the experiments for this study; Y.L., YT.L., XL.T. and WK.L. analyzed the data and wrote the manuscript; XH.Z. and LY.M. helped with the result discussions and writing. All authors reviewed the manuscript.

Availability of data and materials
All GNSS data in the paper can be obtained from the authors upon request but can only be used for academic purposes.

Declarations

Competing interests
Xiaohong Zhang is an editorial board member for Satellite Navigation and was not involved in the editorial review or decision to publish this article. All authors declare that they have no competing interests.

References

Brack, A., Männel, B., & Schuh, H. (2023). Two-epoch centimeter-level PPP-RTK without external atmospheric corrections using best integer-equivariant estimation. *GPS Solutions, 27*(1), 12.

Duong, V., Harima, K., Choy, S., & Rizos, C. (2021). GNSS best integer equivariant estimation using multivariant t-distribution: A case study for precise point positioning. *Journal of Geodesy, 95*, 1–17.

Euler, H.-J., & Schaffrin, B. (1991). On a measure for the discernibility between different ambiguity solutions in the static-kinematic GPS-mode. In *Kinematic systems in geodesy, surveying, and remote sensing: Symposium No. 107 Banff, Alberta, Canada, September 10–13, 1990* (pp. 285–295).

Frei, E. (1990). Rapid static positioning based on the fast ambiguity resolution approach "FARA": Theory and first results. *Manuscripta Geodaetica, 15*, 325–356.

Han, S. (1997). Quality-control issues relating to instantaneous ambiguity resolution for real-time GPS kinematic positioning. *Journal of Geodesy, 71*, 351–361.

Landau, H., & Euler, H.-J. (1992). On-the-fly ambiguity resolution for precise differential positioning. In *Proceedings of the 5th international technical meeting of the satellite division of the Institute of Navigation (ION GPS 1992)* (pp. 607–613).

Li, B. (2018). Review of triple-frequency GNSS: Ambiguity resolution, benefits and challenges. *The Journal of Global Positioning Systems, 16*, 1–11.

Li, B., Shen, Y., Feng, Y., Gao, W., & Yang, L. (2014). GNSS ambiguity resolution with controllable failure rate for long baseline network RTK. *Journal of Geodesy, 88*, 99–112.

Li, T., & Wang, J. (2012). Some remarks on GNSS integer ambiguity validation methods. *Survey Review, 44*(326), 230–238.

Li, Z., Xu, G., Guo, J., & Zhao, Q. (2022). A sequential ambiguity selection strategy for partial ambiguity resolution during RTK positioning in urban areas. *GPS Solutions, 26*(3), 92.

Ma, L., Lou, Y., Lu, L., Liu, W., & Zhu, F. (2022). GNSS best integer equivariant estimation combining with integer least squares estimation: An integrated ambiguity resolution method with optimal integer aperture test. *GPS Solutions, 26*(4), 100.

Miao, W., Li, B., & Gao, Y. (2022). The superiority of multi-GNSS L5/E5a/B2a frequency signals in smartphones: Stochastic modeling, ambiguity resolution, and RTK positioning. *IEEE Internet of Things Journal, 10*(8), 7315–7326.

Odolinski, R., & Teunissen, P. J. (2016). Single-frequency, dual-GNSS versus dual-frequency, single-GNSS: A low-cost and high-grade receivers GPS-BDS RTK analysis. *Journal of Geodesy, 90*(11), 1255–1278.

Odolinski, R., & Teunissen, P. J. (2020). Best integer equivariant estimation: Performance analysis using real data collected by low-cost, single-and dual-frequency, multi-GNSS receivers for short-to long-baseline RTK positioning. *Journal of Geodesy, 94*(9), 91.

Odolinski, R., & Teunissen, P. (2022). Best integer equivariant position estimation for multi-GNSS RTK: A multivariate normal and t-distributed performance comparison. *Journal of Geodesy, 96*(1), 3.

Pisarenko, V., & Rodkin, M. (2010). *Heavy-tailed distributions in disaster analysis* (Vol. 30). Springer.

Takasu, T., & Yasuda, A. (2010). Kalman-filter-based integer ambiguity resolution strategy for long-baseline RTK with ionosphere and troposphere estimation. In *Proceedings of the 23rd international technical meeting of the satellite division of the Institute of Navigation (ION GNSS 2010)* (pp. 161–171).

Tao, X., Liu, W., Wang, Y., Li, L., Zhu, F., & Zhang, X. (2023). Smartphone RTK positioning with multi-frequency and multi-constellation raw observations: GPS L1/L5, Galileo E1/E5a, BDS B1I/B1C/B2a. *Journal of Geodesy, 97*(5), 43.

Teunissen, P. J. (1993). Least-squares estimation of the integer GPS ambiguities. In *Invited Lecture, Section IV Theory and Methodology, IAG General Meeting, Beijing, China* (pp. 1–16).

Teunissen, P., Joosten, P., & Tiberius, C. (1999). Geometry-free ambiguity success rates in case of partial fixing. In *Proceedings of the 1999 national technical meeting of the Institute of Navigation* (pp. 201–207).

Teunissen, P. J. (1998). Success probability of integer GPS ambiguity rounding and bootstrapping. *Journal of Geodesy, 72*, 606–612.

Teunissen, P. (2003a). Integer aperture GNSS ambiguity resolution. *Artificial Satellites, 38*(3), 79–88.

Liu *et al. Satellite Navigation*   (2024) 5:12

Page 16 of 16

Teunissen, P. (2003b). Theory of integer equivariant estimation with application to GNSS. *Journal of Geodesy, 77*(7–8), 402–410.

Teunissen, P. (2005a). GNSS ambiguity resolution with optimally controlled failure-rate. *Artificial Satellites, 40*(4), 219–227.

Teunissen, P. (2005b). On the computation of the best integer equivariant estimator. *Artificial Satellites, 40*(3), 161–171.

Teunissen, P. (2020). Best integer equivariant estimation for elliptically contoured distributions. *Journal of Geodesy, 94*(9), 82.

Teunissen, P. J., & Verhagen, S. (2009). The GNSS ambiguity ratio-test revisited: A better way of using it. *Survey Review, 41*(312), 138–151.

Teunnissen, P. (1995). The least-square ambiguity decorrelation adjustment: A method for fast GPS integer ambiguity estimation. *Journal of Geodesy, 70*(1), 65–82.

Tiberius, C., & De Jonge, P. (1995). Fast positioning using the LAMBDA method. In: *Proceedings DSNS-95, Paper* (Vol. 30, No. 8).

Verhagen, S., & Teunissen, P. (2005). Performance comparison of the BIE estimator with the float and fixed GNSS ambiguity estimators. In *A window on the future of geodesy: Proceedings of the international association of geodesy IAG general assembly Sapporo, Japan June 30–July 11, 2003* (pp. 428–433).

Verhagen, S., Li, B., & Teunissen, P. J. (2013). Ps-LAMBDA: Ambiguity success rate evaluation software for interferometric applications. *Computers & Geosciences, 54*, 361–376.

Vollath, U., & Talbot, N. C. (2013). *GNSS signal processing methods and apparatus with candidate set selection*. Google Patents.

Wang, J., Stewart, M., & Tsakiri, M. (1998). A discrimination test procedure for ambiguity resolution on-the-fly. *Journal of Geodesy, 72*, 644–653.

Wang, L., Feng, Y., & Guo, J. (2017). Reliability control of single-epoch RTK ambiguity resolution. *GPS Solutions, 21*, 591–604.

Wu, Z., & Bian, S. (2015). GNSS integer ambiguity validation based on posterior probability. *Journal of Geodesy, 89*, 961–977.

Xu, P., Shi, C., & Liu, J. (2012). Integer estimation methods for GPS ambiguity resolution: An applications oriented review and improvement. *Survey Review, 44*(324), 59–71.

Yang, Y., Zhou, F., & Song, S. (2024). Improving precise point positioning (PPP) performance with best integer equivariant (BIE) estimator. *GPS Solutions, 28*(1), 50.

Yu, X., Xia, S., & Gao, W. (2021). A practical method for calculating reliable integer float estimator in GNSS precise positioning. *Survey Review, 53*(377), 97–107.

Zhang, J., Wu, M., Li, T., & Zhang, K. (2015). Integer aperture ambiguity resolution based on difference test. *Journal of Geodesy, 89*, 667–683.

Zhang, Z., Li, X., & Yuan, H. (2023). Best integer equivariant estimation based on unsupervised machine learning for GNSS precise positioning and navigation in complex environments. *IEEE Transactions on Aerospace and Electronic Systems.* https://doi.org/10.1109/TAES.2023.3320115

Zhang, Z., Yuan, H., He, X., Li, B., & Geng, J. (2023). Best integer equivariant estimation with quality control in GNSS RTK for canyon environments. *IEEE Transactions on Aerospace and Electronic Systems., 59*, 4105.

Zhu, N., Marais, J., Bétaille, D., & Berbineau, M. (2018). GNSS position integrity in urban environments: A review of literature. *IEEE Transactions on Intelligent Transportation Systems, 19*(9), 2762–2778.

Publisher's Note

Ying Liu   received the bachelor's degree in navigation engineering from the School of Geodesy and Geomatics, Wuhan University, Wuhan, China, in 2022, where he is currently pursuing the master's degree. His current research interests include low-cost GNSS/INS integrated navigation and its applications.

Dr. Wanke Liu   is currently a professor at Wuhan University, China. He obtained his B.Sc., M.Sc., and Ph.D. degrees in Geodesy and Engineering Surveying at the School of Geodesy and Geomatics at Wuhan University in 2001, 2004, and 2008. His main research interests include precise positioning technology of GNSS, low-cost multi-sensor integration technology, and autonomous orbit determination of navigation satellites.

Dr. Xiaohong Zhang   is currently a professor at Wuhan University. He obtained his B.Sc., M.Sc., and Ph.D. degrees with distinction in Geodesy and Engineering Surveying from Wuhan University in 1997, 1999, and 2002, respectively. His main research interests include PPP, PPP-RTK, GNSS/INS integration technology, and its applications.

Yantao Liang   received the bachelor's degree in navigation engineering from the School of Geodesy and Geomatics, Wuhan University, Wuhan, China, in 2022, where he is currently pursuing the master's degree. His current research interests include low-cost GNSS/INS integrated navigation and its applications.

Xianlu Tao   is currently a lecturer at the School of Instrument Science and Engineering, Southeast University, China. He received his B.S.C., M.S.C., and Ph.D. degrees in Geodesy and Engineering Surveying from the School of Geodesy and Geomatics of Wuhan University in 2016, 2019, and 2023, respectively. His primary areas of research are GNSS high-precision positioning, multi-sensors integrated navigation, and its applications.

Liye Ma   received his B.S.C., M.S.C., and Ph.D. degrees in Geodesy and Engineering Surveying from the School of Geodesy and Geomatics of Wuhan University in 2016, 2019, and 2023. His current research mainly focuses on GNSS ambiguity resolution and high-precision GNSS/SINS integrated navigation.